Deformation, Twinning and Thermo-Mechanical Strengthening of Ti50Ni47Fe3

Moberly, Proft, Duerig, Sinclair

Acta metall. mater
Vol. 38, Nr. 12
pp. 2601-2612

1990

Acta metall. mater. Vol. 38, No. 12, pp. 2601–2612, 1990
Printed in Great Britain. All rights reserved
0956-7151/90 $3.00 + 0.00

DEFORMATION, TWINNING AND THERMO-MECHANICAL STRENGTHENING OF $Ti_{50}Ni_{47}Fe_3$

W. J. MOBERLY[1], J. L. PROFT[2], T. W. DUERIG[2] and R. SINCLAIR[3]

[1]Department of Materials Science and Engineering, Stevens Institute of Technology, Castle Point on the Hudson, Hoboken, NJ 07030, [2]Raychem Corporation, Menlo Park, CA 94025, [3]Department of Materials Science and Engineering, Stanford University, Stanford, CA 94305, U.S.A.

(*Received* 26 *March* 1990)

Abstract—The dislocation Burgers vectors for the B2 intermetallic compound, $Ti_{50}Ni_{47}Fe_3$, are shown to be the ⟨010⟩ type, which provide this alloy with only three independent slip systems. However, concurrent dislocation slip and mechanical twinning on {114} planes affords the polycrystalline material with greater than 50% room temperature ductility. Individual twins do not grow greater than 50–150 nm in width, and the twinning density increases with the extent of cold working. Annealing a cold worked structure, comprised of mechanical twins and dislocations, results in the formation of subgrains with a size limited by the width of the twins. Greater cold working produces a finer twin spacing and, subsequently after annealing, a refined subgrain size which in turn brings about an improved combination of yield strength and ductility.

Résumé—On montre que les vecteurs de Burgers des dislocations du composé intermétallique B2, $Ti_{50}Ni_{47}Fe_3$, sont du type ⟨010⟩, ce qui donne à cet alliage seulement trois systèmes de glissement indépendants. Cependant, le glissement des dislocations combiné avec le maclage mécanique sur des plans {114} procure au matériau polycristallin une ductilité supérieure à 50% à la température ambiante. La croissance des macles individuelles conduit à des largeurs maximales de 50 à 150 nm et la densité de macles augmente avec le degré d'écrouissage à froid. Le recuit d'une structure écrouie à froid, formée de macles mécaniques et de dislocations, a pour résultat la formation de sous-grains dont la taille est limitée par l'épaisseur des macles. Un écrouissage à froid plus important conduit à un espacement des macles plus réduit et par conséquent, aprés recuit, à un affinement de la taille des sous-grains, ce qui améliore à son tour la résistance mécanique et la ductilité.

Zusammenfassung—Es wird gezeigt, daß der Bergersvektor der Versetzungen in der intermetallischen Verbindung $Ti_{50}Ni_{47}Fe_3$ vom ⟨010⟩-Typ ist. Diese Legierung besitzt daher nur drei unabhängige Gleitsysteme. Allerdings geben gleichzeitige Gleitung und mechanische Zwillingsbildung auf {114}-Ebenen dem polykristallinen Material eine Duktilität von mehr als 50% bei Raumtemperatur. Die einzelnen Zwillinge werden nicht breiter als 50–150 nm; mit zunehmender Verformung steigt die Dichte dieser Zwillinge. Wird eine solche Verformungsstruktur, bestehend aus Versetzungen und mechanischen Zwillingen, ausgeheilt, dann bilden sich Subkörner in einer Größe, die durch die Breite der Zwillinge begrenzt ist. Stärkere Verformung ergibt Kleinere Zwillingsabstände und nach dem Ausheilen eine verfeinerte Subkorngröße. Diese Wierderunm verbessert Fließfestigkeit und Duktilität.

INTRODUCTION

Ordered intermetallic compounds represent an interesting class of alloys with potential applications at high temperatures. One particular difficulty in their development concerns their notorious brittleness compared to conventional metallurgical alloys. The strong interatomic bonding associated with high-temperature stability often precludes room and low-temperature plasticity. TiNi alloys constitute an intriguing anomaly to this general behavior. While being well-known for their shape memory properties, involving a reversible low-temperature phase transformation [1–5], the high temperature B2 phase can undergo significant plastic deformation, which is, of course, useful for forming operations. In this article we describe a detailed study of the deformation mechanisms of a TiNi based alloy and show how thermo-mechanical processing can be used to produce material with high strength and ductility.

Intermetallics generally have limited ductility at room temperature [6–8] owing to their few and difficult slip systems, with Burgers vectors greater than atomic, nearest neighbor distances. However, TiNi alloys have been found to undergo mechanical twinning during deformation [9], which suggests an alternative mode of deformation to dislocation slip. (It should be noted that this twinning process is quite distinct from martensitic transformation twinning, even when stress-induced.) As we shall describe, a combination of slip and twinning is responsible for up to 50% ductility for TiNi, which far exceeds that of other B2 alloys. This is apparently the only material which has been investigated for this combination of deformation modes.

Transmission electron microscopy (TEM) is utilized in this study to evaluate the twinning and slip systems, as well as to characterize the substructure developed for different mechanical processing conditions. The deformation modes are analyzed with respect to the number of independent slip systems (ISS), since five ISS is generally the accepted requirement for compatible polycrystalline ductility. During thermo-mechanical processing (and annealing) the interaction of dislocations and mechanical twins results in the formation of subgrains. The fine size of the subgrains is directly influenced by the submicron size of the mechanical twins and in turn results in improved mechanical properties.

EXPERIMENTAL

Ternary TiNiFe alloys are similar to the binary TiNi compound except for Fe being substituted for Ni during casting. Although $Ti_{50}Ni_{47}Fe_3$ has the same crystal structures as the binary alloy (both cubic B2 at high temperatures and monoclinic B19′ at low temperatures), the martensitic transformation temperature is lowered to well below room temperature. Cold working (20°C) cannot stress-induce the martensitic transformation. Fully annealed (2 h at 875°C) half-inch diameter round bars were swaged at room temperature to achieve reduction of areas of 10, 20, 30, and 40%. (The importance of starting with "fully" annealed material stems from the fact that once a substructure is developed in this alloy, it is quite stable. Previous working to form the original 1/2″ bars develops such a substructure.) Each cold working process was followed by various recovery anneals; 400, 500, and 600°C for 1, 10, 100, and 1000 min, respectively. The various temperatures and durations of annealing were chosen to help determine how microstructures evolve and which processing conditions produce the desired strengthening. Additional bars were warm swaged at 500°C, followed by various recovery anneals.

Tensile tests were performed using an MTS model 810 on the fully annealed, as-worked, warm-worked, and heat-treated material, with the tensile axis parallel to the swaging axis. (The 3% Fe also ensures that martensite will not be induced during machining of tensile specimens.) As discussed by Proft [10], thermo-mechanical processing for this alloy, working followed by annealing, results in improved mechanical properties.

The above processed samples were observed with Philips EM400 and EM430 microscopes. TEM samples were prepared by electropolishing foils in an electrolyte of 75 vol.% methanol—25 vol.% nitric acid at −15°C and 12 V [11]. In order to provide an appropriate comparison of microstructures, all TEM micrographs were obtained of samples that were carefully sectioned transverse to the swaging direction, such that the swaging axis is always normal to the TEM thin foils. An exception is Fig. 4, which exhibits a foil sectioned longitudinally. No martensitic transformation was introduced by TEM sample preparation.

RESULTS

Microstructural characterization

The fully annealed condition, depicted in Fig. 1, exhibits few dislocations ($<1\times10^9/cm^2$) and a nominal grain size of 40 μm, as determined by optical microscopy (not presented). A tensile bar elongated 1% at room temperature displays dislocations and no stacking faults. Figure 2(a–c) are bright field images obtained under different two-beam conditions. Dislocations within the parallel slip bands in Fig. 2(b) are invisible in Fig. 2(a) and (c). (Note small arrows in Fig. 2.) The dislocations in Fig. 2 are determined to have Burgers vectors of the type $\mathbf{b} = [\mathbf{010}]$, consistent with those observed by Pelton [12]. The 10% cold worked bar exhibits many dislocations ($1–2\times10^{11}/cm^2$), indicating the unusual ductility of this particular intermetallic compound (Fig. 3). The entangled nature of the dislocations after 10% deformation, and the narrow bend contours inherent to deformed TiNi TEM foils, precludes definitive analysis that all dislocations are $\mathbf{b} = [\mathbf{010}]$ type.

An occasional grain in the 10% cold swaged bar exhibits, via TEM imaging, a few mechanically induced twins; which have the same crystal structure, based on electron diffraction, as the parent material (i.e. they are not related to martensitic transformation twins). By longitudinally sectioning the 10%

Fig. 1. Bright field image of microstructure of $Ti_{50}Ni_{47}Fe_3$ alloy after annealing 2 h at 875°C. The nominal grain size is ~40 μm.

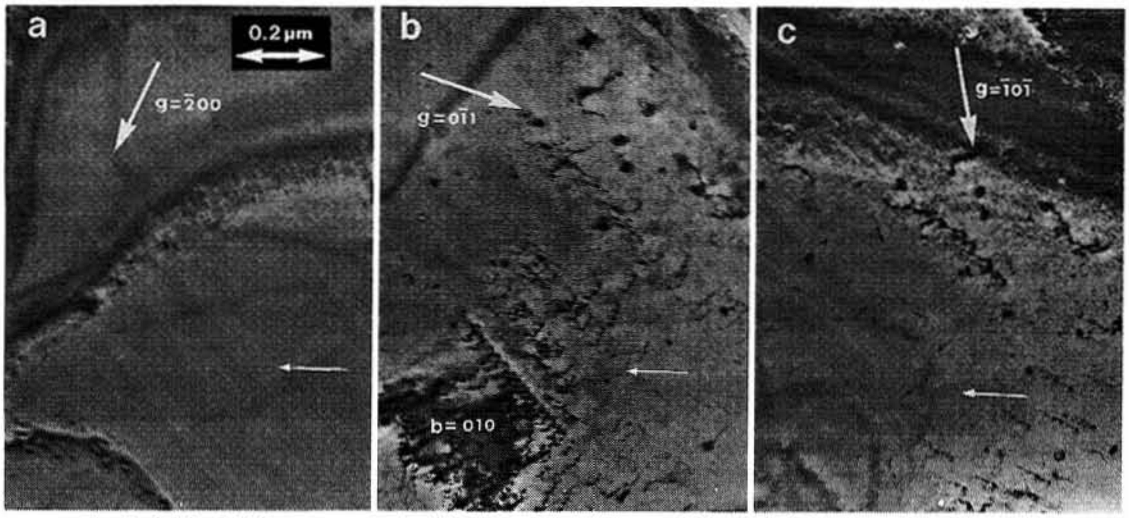

Fig. 2. Bright field images acquired, with different two-beam conditions, of dislocations after 1% plastic strain. Note the same slip bands are indicated by the small arrows in each micrograph. The dislocations are determined to be of the type $b = \langle \mathbf{010} \rangle$.

cold worked bar and fiducially marking the TEM sample, the twinning plane is observed as being 40° (±5°) to the swaging direction [Fig. 4(a)]. Electron diffraction [Fig. 4(b)] and a schematic of a twinned diffraction pattern [Fig. 4(c)] indicate that the twinning occurs on {114} planes.

Whereas more extensive cold working produces a higher dislocation density, a more notable difference is the increase in twin density as a result of added deformation. Figures 5(a) and 5(b) of the 30% cold worked bar illustrate both a higher dislocation density ($2–4 \times 10^{11}/cm^2$), as compared to the 10% cold

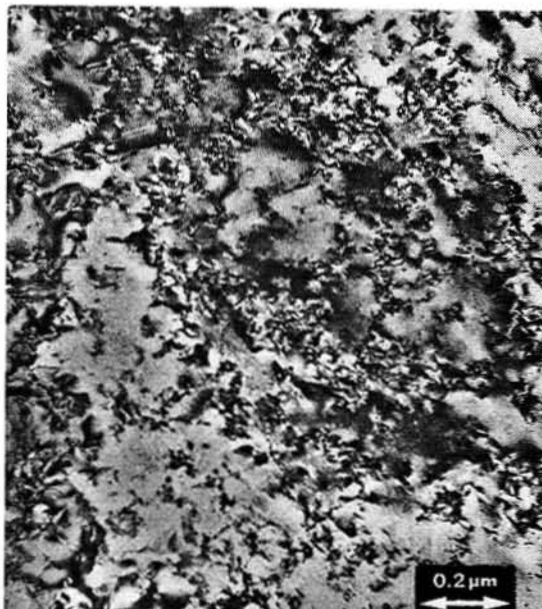

Fig. 3. Bright field image of typical dislocated structure after 10% cold work via swaging.

worked material, and a higher twin density, with twins present throughout many of the grains. In addition, electron diffraction patterns [Fig. 5(c)] of one micron diameter areas within many different grains exhibit similar matrix–twin crystal orientation relationships. $\{\bar{1}\bar{1}1\}$ and {110} orientations of the matrix and twin are almost parallel to each other and are within 10–15° of the normal of the transverse section, i.e. the swaging direction of the bar. These preferred orientations are an indication of {114} twinning [13] and, as shall be discussed later, of grain rotation during deformation. The 40% cold worked sample exhibits most grains as having a uniform twin density throughout each individual grain (Fig. 6). The primary differences between the 30 and 40% cold worked samples are more and closer spaced twins, indicative of a higher percentage of twinned material in the latter. The total percentage of twinned material in a grain increases with extent of deformation. Less than five per cent of the volume is twinned for the 10% cold worked material, increasing to about twenty per cent for the 30% cold worked sample (Fig. 5) and to nearly forty percent for the 40% cold worked material (Fig. 6). (The scale of the twins is too small for adequate analysis by optical microscopy.)

Figure 7 schematically describes how the twins are arranged in the matrix of a deformed grain. In the sample of only 10% deformation (Fig. 4), the majority of the grain is presumed to be the untwinned matrix. Thus every alternating region may be properly labelled as a "twin". In Fig. 4 the twins are confined to a band less than 1 micron wide that runs the entire length (at a 45° angle) of the grain. Each individual twin does not necessarily traverse the entire length of the grain. However, a second twin initiates near where the first twin ends, such that the band has twins continuing throughout its length.

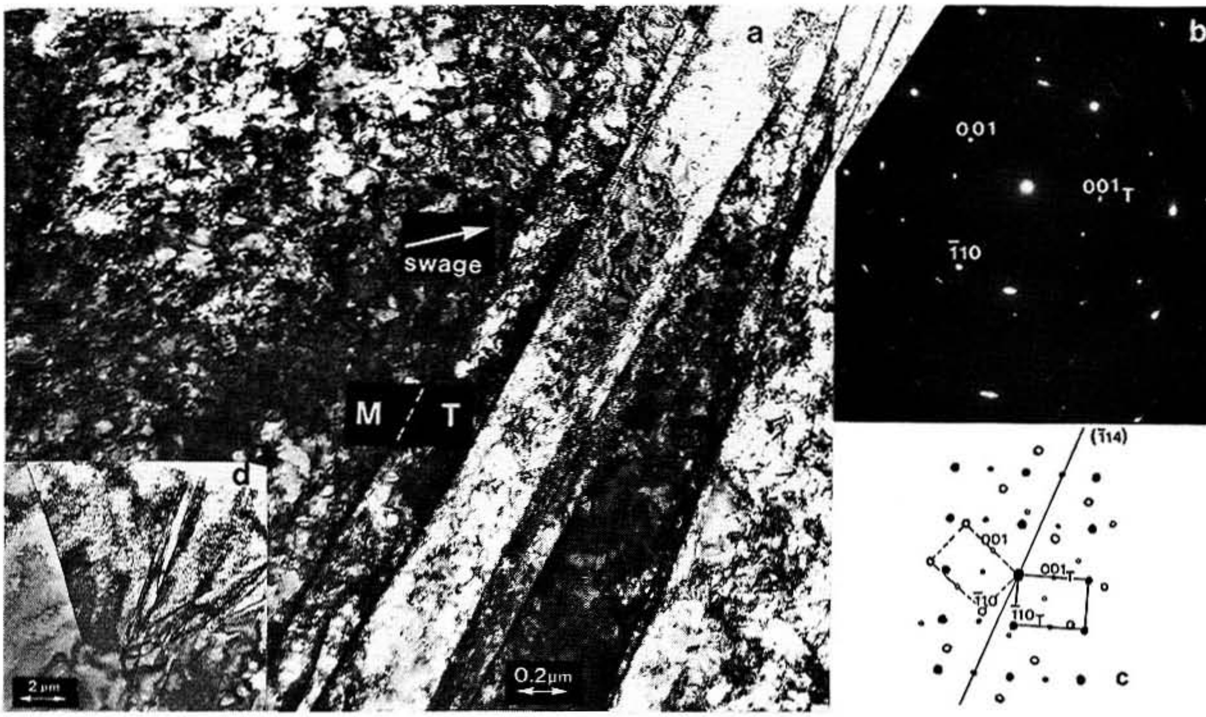

Fig. 4. (a) Bright field image of grain with a few mechanical twins after 10% cold work. This longitudinal section indicates the swaging direction. (b) [110] zone axis electron diffraction pattern exhibiting $\{\bar{1}14\}$ deformation twinning. (c) Schematic drawing of figure (b). (d) Low magnification image indicating the twins to be confined to a narrow slip band that extends across the grain.

Although the intermediate untwinned matrix regions may vary considerably in width, the widths of the twinned regions are nominally 50–300 nm, as directly measured in Fig. 4 with the twinning plane normal to the image.

Parallel twins, with generally one set of twin planes in each grain, are observed throughout the "width" of the grains of the 30 and 40% deformed bars (see Figs 5–7). Accounting for a correction factor for sectioning, most of the alternating layers of twin and

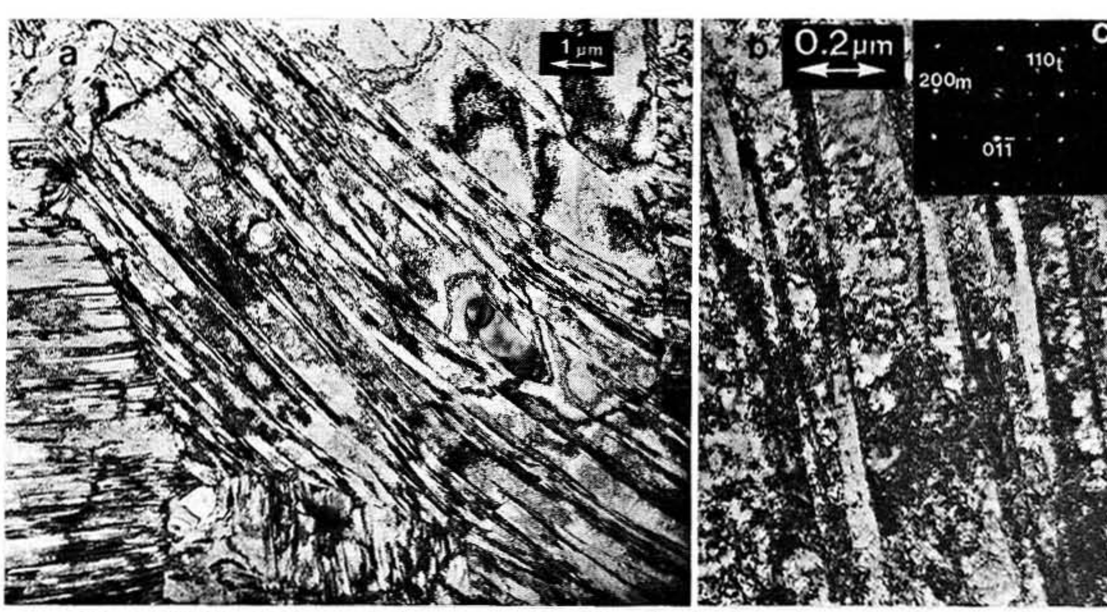

Fig. 5. (a) Bright field image of microstructure after 30% cold work via swaging, sectioned transversely. (b) Higher magnification image indicating typical dislocation density and twin density has increased as compared to Fig. 3. (c) [110] and $[1\bar{1}\bar{1}]$ zone axis electron diffraction patterns of matrix and twin respectively, indicative of {114} twinning [14].

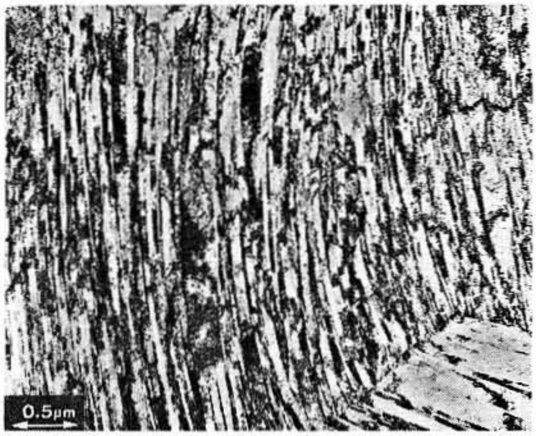

Fig. 6. Bright field image of microstructure after 40% cold work via swaging, exhibiting a finer twin density as compared to Fig. 5.

matrix are nominally 30–120 nm in the 30% deformed sample and 30–80 nm for the 40% cold worked material. Again each twin does not extend the entire "breadth" of the grain; however, where one twin ends, a second twin generally starts, and bands of twins extend the breadth of the grain (see Figs 5–7). Where twins in one grain intersect a grain boundary, twins usually exist in the next grain, impinging the grain boundary at a different angle.

For a sample having primarily dislocations after cold deformation, annealing results in recovery via dislocation annihilation. Figure 8(a) and 8(b) depict the microstructures of the 10% cold worked material

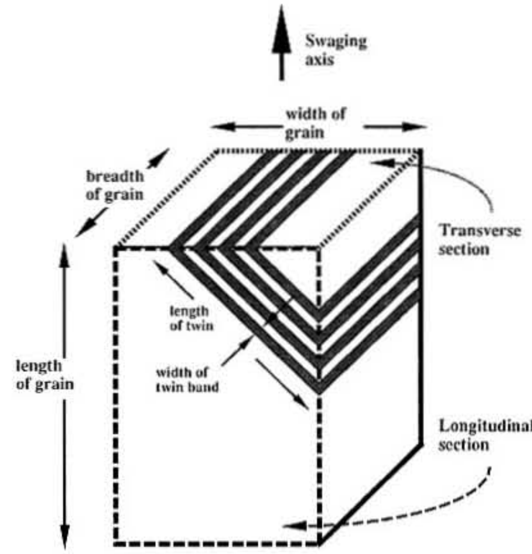

Fig. 7. Schematic drawing of typical grain after mechanical twinning due to swaging, which defines the nomenclature used to the describe microstructure of various samples. Dark bands represent "slip bands of twins" that extend across the grain, although an individual twin may not. All micrographs are of transverse sections, except Fig. 4 which is of a longitudinal section.

following a 10 min anneal and a 1000 min anneal at 500°C, respectively. Where dislocations do align during annealing, the substructure is not stable, as the spacing between rows of dislocations increases with subsequent annealing. However, heat treatment of the 30% cold worked material evolves a distinctly

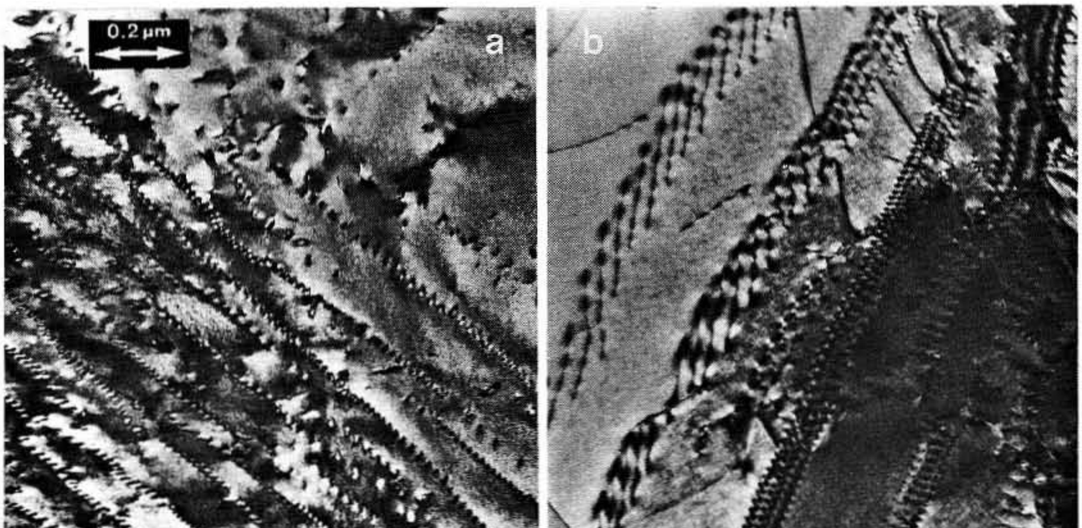

Fig. 8. Bright field image of microstructure after annealing the 10% cold worked material for 10 min at 500°C. Recovery occurs primarily via dislocation annihilation, as compared to Fig. 3, with selected areas exhibiting dislocation alignment. (b) Further annealing (1000 min at 500°C) results in additional dislocation annihilation and greater separation between rows of dislocations.

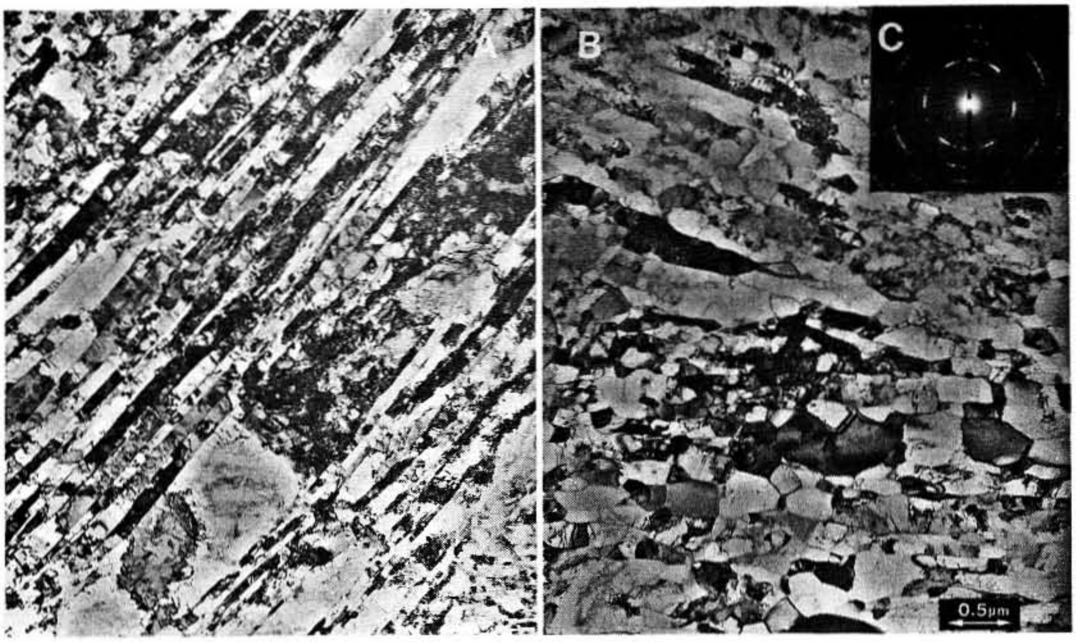

Fig. 9. Bright field image of microstructure after annealing the 30% cold worked material for 10 min at 500°C. Recovery has little effect on the twin boundaries, as compared to Fig. 5. (b) Further annealing (1000 min at 500°C) results in the development of a fine, stable substructure. (c) Electron diffraction indicates the presence of subgrains with twin-related orientations.

different microstructure. A 10 min anneal at 500°C, although reducing the dislocation density, does not have much effect on the twin boundaries [Fig. 9(a)]. After a 1000 min anneal [Fig. 9(b)], a fine substructure has developed with a size comparable to the twin spacing. Although a twinned microstructure is not readily evident in the image, electron diffraction indicates the twinned orientation relationship is still present [Fig. 9(c)]. Regions of the substructure in the same "row" (a "row" being defined by previous twin boundaries) exhibit only a slight relative rotation ($\sim 5°$) in the diffraction pattern indicative of subgrains rather than a random, recrystallized, fine grain structure. In addition, regions in neighboring "rows" exhibit relative orientations indicative of the twinned orientations that were observed in Fig. 5(c).

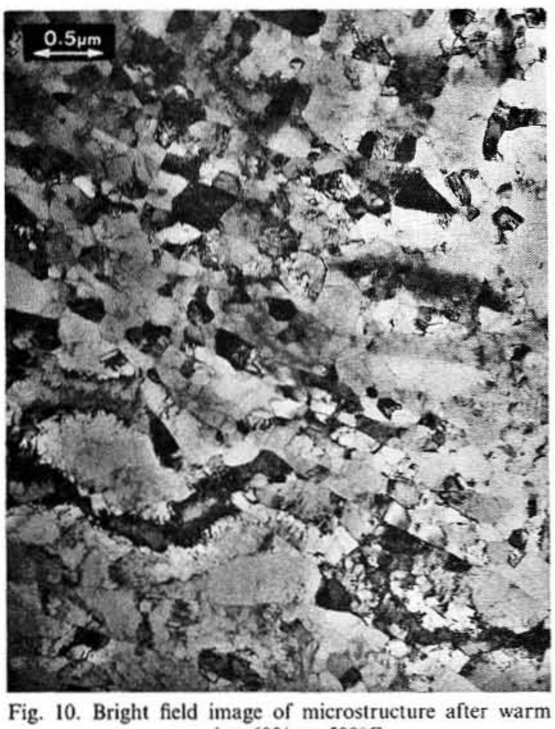

Fig. 10. Bright field image of microstructure after warm swaging 60% at 500°C.

The 60% warm-swaged (500°C) bar exhibits a fine as-worked substructure. The directional texture in Fig. 10 suggests that mechanical twinning is occurring during warm working. If mechanical twinning occurs during warm working, recovery while the temperature is still high would subsequently result in subgrain formation (prior to the observation of Fig. 10). Although electron diffraction suggests a (114) twinning plane, whether or not this material really did mechanically twin during warm working is not absolutely determined for this sample. (Deformation twinning during warm working has been observed, and the possible twinning systems that exist are currently being studied [14].) The microstructure of the warm-worked material does not change significantly upon annealing at 500°C.

Mechanical properties

The yield strengths and ductilities of fully annealed, as-worked, and heat treated samples are listed in Table 1. The fully annealed material exhibits a yield strength of ~ 400 MPa and greater than 30% tensile elongation to failure (Fig. 11). This strength is

Table 1. Mechanical properties of worked and annealed samples

	Work condition	Heat treatment	Yield strength (MPa)	Elongation (%)
A	"fully annealed"	2 h at 875°C	410	30–50
B	10% cold swage	No H.T.	690	13
C	10%	10 min at 400°C	650	26
D	10%	10 min at 450°C	560	25
E	10%	1 min at 500°C	555	32
F	10%	10 min at 500°C	510	26
G	10%	100 min at 500°C	500	30
H	30% cold swage	No H.T.	1030	7
I	30%	10 min at 350°C	840	17
J	30%	10 min at 400°C	800	13
K	30%	10 min at 450°C	750	20
L	30%	1 min at 500°C	740	25
M	30%	10 min at 500°C	700	22
N	30%	100 min at 500°C	660	25
O	30%	1000 min at 500°C	640	30
P	30%	10 min at 550°C	630	31
Q	30%	10 min at 600°C	580	31
R	40% cold swage	No H.T.	1090	4
S	40%	10 min at 400°C	850	29
T	40%	10 min at 500°C	730	24

slightly greater than that of low-carbon steel, and much greater than the strength of typical, brittle intermetallics (Ni_3Al, TiAl, and NiAl). By cold working up to 30%, the yield strength is increased to above 1000 MPa, while reducing the ductility to ~5%. Figure 12(a) plots the yield strength and ductility of the 30% cold worked material as a function of annealing time at 500°C. A one-minute anneal reduces the yield strength, but to a value still almost double that of the fully annealed alloy. Meanwhile the ductility is substantially improved to ~30%. As seen from the micrographs and to be discussed in Section "e", annealing the cold worked structure develops a fine substructure to which is attributed the improved mechanical properties. Longer anneals do not dramatically change the mechanical properties further. The values of yield strength and ductility for the different annealing conditions listed in Table 1 are plotted in Fig. 12(b). As expected, a longer and/or higher temperature anneal results in a lower yield strength and greater ductility. The heat treating of the more severely cold worked material results in a higher combined yield strength and ductility. In addition, annealing the warm worked material does not significantly change its mechanical properties.

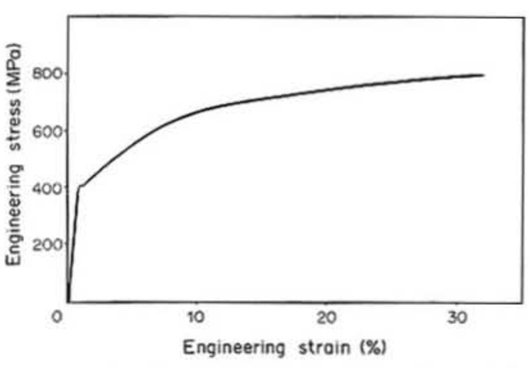

Fig. 11. Engineering stress vs engineering strain graph for fully annealed tensile sample of $Ti_{50}Ni_{47}Fe_3$. Elongation to failures of up to 50% have been observed.

DISCUSSION

(a) Dislocations in B2 intermetallic alloys

In order to understand the importance of mechanical twinning and the influence of twinning on thermo-mechanical strengthing, the nature of dislocations in TiNi must first be discussed. Dislocation motion is generally not easy in intermetallics [15], as the ordered superlattices necessitate larger Burgers vectors for the dislocations, which are often dissociated [16]. Thus the significant multiplication of dislocations observed in cold-worked TiNi is unusual. Still, plastic deformation, via dislocation motion alone, is difficult in TiNi. For the B2 superlattice the smallest Burgers vector is of the type $\mathbf{b} = [\mathbf{010}]$, so that the passage of a dislocation does not disorder the structure [17]. The $\langle 010 \rangle$ dislocations observed in this study (Fig. 2) are consistent with the $\langle 010 \rangle \{101\}$ slip system reported by Pelton [12] both after straining tensile samples 5% at room temperature and after thermal cycling samples under an applied load. $\langle 010 \rangle$ type dislocations, independent of their glide planes, provide for only three independent slip systems (ISS), which are insufficient for compatible plastic deformation of a polycrystalline material [18, 19]. Studies of other B2 materials have shown additional slip systems active in single crystals deformed at room temperature [20, 21] and in polycrystalline samples deformed at high temperature [22, 23]. However, these alloys do not have such extensive ductility as TiNi. (The lack of TEM analysis in some of these studies precluded observation of the fine detail of the microstructure and deformation mechanisms.) Since plastic deformation cannot readily occur by means of $\langle 010 \rangle$ slip alone, mechanical twinning offers an alternative or additional means of deformation. As is indicated by the concomitant increase in both dislocation density and twin density with an increase in cold working, twin systems accommodate for the deficient dislocation slip systems. This will be discussed in more detail in Section "d".

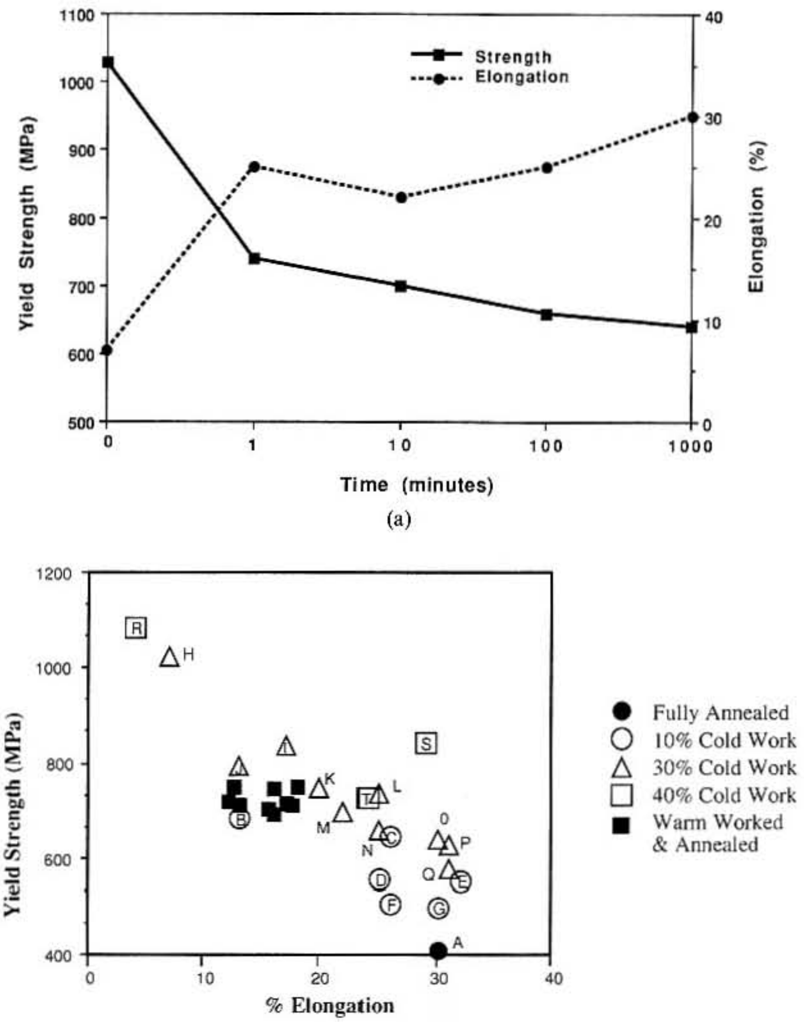

(b)

Fig. 12. (a) Graph of yield strength (solid line) and ductility (dotted line) vs duration of annealing at 500°C for sample having experienced 30% cold work prior to annealing. (b) Graph of yield strength vs ductility for different work and annealing conditions (see Table 1 for sample conditions).

(b) {114} Twinning

All the observed mechanical twins are determined to have a {114} twinning plane, one of the twinning modes deduced by Goo [9] for this alloy. As discussed by Goo, twinning on (114) planes involves atoms undergoing a shear strain of 0.707 in the $[22\bar{1}]$ direction. In order to preserve the B2 structure, Goo's model involves half the atoms, on alternating (110) planes, shuffling $0.5a_0$ in the $[00\bar{1}]$ direction. Twinning which requires shuffling as well as shearing is considered to be a complex twinning mechanism as discussed by Laves [24]. This shuffling recreates the B2 structure from the mechanical twin region without requiring atoms to have to "pass over" each other. Since the resulting twin has the same structure as that of the original matrix, these twins may be described as "true" twins rather than pseudotwins [25], which have also been observed in this alloy [9].

Knowledge of the swaging direction enables exact identification of the direction of twinning shear. Although Goo's model involved a shear in the $[22\bar{1}]$ direction followed by shuffling on (110) planes, it would also be possible to have (114) twinning with a reverse shear in the $[\bar{2}\bar{2}1]$ direction followed by shuffling on $(\bar{1}\bar{1}2)$ planes in $\langle\bar{1}\bar{1}\bar{1}\rangle$ directions. Many modes of mechanical twinning may be possible [26]. The magnitude of the shear, the plane of shearing, the magnitude of the shuffle, the direction of shuffle, the fraction of atoms that shuffle, and the relative closeness of atoms during shuffling must all be considered. Sometimes the magnitude of the shear may be increased in order to allow "easier" shuffling [14]. However, for the case of swaging in Fig. 4, it is readily shown that the maximum shear stress present is in the $[22\bar{1}]$ direction and produces (114) twinning as in the model of Goo.

Goo and others [26, 27, 28] determined that mechanical twinning on various (114) type planes may provide for sufficient independent slip systems for plastic deformation without the need of dislocation slip systems. Unlike dislocation slip, where the same slip system is activated for either positive or negative shear, a mechanical twin can only form due to a shear in a particular direction [29]. Whereas five (5) ISS for dislocations are required for plastic deformation [18], deformation of polycrystalline materials via mechanical twinning alone may necessitate the activation of more than five twinning systems. There are twelve $\{114\}\langle 22\bar{1}\rangle$ twinning systems; of these., however, only six independent twinning systems need be activated to produce an arbitrary shape change in a single crystal [28].

The longitudinal section of a sample with only few twins (Fig. 4) provides for direct observation of the twinning plane. Since the twinning plane is at $\sim 45^\circ$ to the swaging direction, the shearing is occurring on the particular (114) plane with maximum resolved shear stress. Most TEM observations, however, were made of transverse sections, in order to compare relative microstructural differences for different extents of deformation. As discussed previously by Moderly [13], (110) and $(\bar{1}\bar{1}1)$ (twin and matrix) zone axes being approximately parallel implies the twinning plane to be the (114) plane, as opposed to the (112) plane, which is the twin plane typical for b.c.c. metals and for pseudotwinning in TiNi [9]. In addition, the observation that these zone axis orientations are within 10–15° of the swaging direction (normal to the TEM foil) infers that the (114) twinning is occurring on a (114) plane that is close to 45° from the swaging direction.

Although deformation twinning involves shearing on the particular (114) plane with the highest resolved shear stress, whether [30] or not [31] twinning involves a Critical Resolved Shear Stress (CRSS) is a subject of debate. Thus far, a CRSS for twinning has never been measured and/or calculated as has been done for dislocation motion using a Peierls stress criterion [32]. Speculation as to the presence (or lack) of a CRSS for twinning and twinning being "strain-controlled" is discussed in Section (d) and in another study [33].

(c) *Twin density vs extent of deformation*

Samples subjected to more deformation show a greater density of twins. The percentage of twinned material is expected to increase with deformation in a system where deformation twinning occurs. In many material systems further mechanical twinning may be accommodated by the growth of the individual twins. Nucleation of the twin is often the main barrier to deformation by twinning. The growth of the twin correlates with the increase in plastic strain and even sometimes occurs at a lower stress. However, in polycrystalline TiNiFe new twins are nucleated as deformation is increased. Apparently a newly nucleated twin quickly grows to a particular size and then remains stable with further deformation, while new twins are formed. Continued growth of a twin may be restricted by the confines of the grain boundary and the surrounding grains, as well as by other nearby twins.

The observation that some twins neither "start" nor "end" at a grain boundary, in this study as well as in the study by Goo [9], indicates that twins may not have to nucleate at grain boundaries. This may be a sectioning problem, whereby the particular grain boundary of intersection is not imaged in the TEM section. In this study, however, bands of twins are found to extend across the breadth and length of the grain. When a twin does impinge a grain boundary, an accommodating twin may be expected to nucleate in the adjacent grain at the grain boundary. Where two twins (in Figs 4–7) have ends that meet, the two twins appear to have nucleated separately and then grown to impinge each other to accommodate the shearing of that "twin band". The formation of twins within a "band" may be compared to slip bands that occur for dislocations, with a band of sheared material extending throughout the grain. Rather than this band widening with further deformation, additional twins shear a neighboring region and form a new twin band.

The stress state within a particular grain is not constant during a swaging operation. In fact, the stress could change such that a previously formed twin might not be stable, with regions of local detwinning occurring. Yet as the grain shape is constantly elongating along the swage direction, and as only one set of twin planes is usually observed in any one grain, complete detwinning and renucleation of new twins can be presumed not to occur. Moreover, the typical twin, after forming, does not decrease in size with subsequent deformation. The average twin width may decrease slightly with subsequent deformation, because the initial twins may give rise to internal stresses that cause later twins to be slightly smaller. The width of the smallest twins is approximately the same for the 10, 30, and 40% deformed samples (30–50 nm), as observed in Figs 4, 5, and 6, respectively. The upper limit of the "twin" sizes appears to decrease from 120 to 80 nm as deformation increases from 30 to 40%, but this apparent inconsistency can be attributed to the difficulty in differentiating between twinned and untwinned (matrix) regions in the heavily deformed samples.

As noted in the Microstructural Characterization section, the percent twinned material, or total twin density, increases with deformation. For the 10, 30, and 40% cold worked samples the twin densities are less than 5%, 20% and 40%, respectively. Although twinning on (114) planes involves a significant shear strain of 0.707, these twinning densities are not sufficient by themselves to account for all of the deformation. A twin density of five percent involving a shear of 0.707 on a plane at 45° to the swaging direction, would only result in an elongation of

~2%. Thus most of the 10% deformation is accounted for by dislocation motion. This is in agreement with the dislocation multiplication, from $< 1 \times 10^9/cm^2$ to $\sim 1 \times 10^{11}/cm^2$, observed during the first 10% deformation. Likewise the twin densities in the 30 and 40% deformed samples account for less than half of the elongation, although the twinning accounts for an increasing percentage of the deformation at higher strains. As previously mentioned, twinning and dislocation motion occur concurrently; the twinning provides a second deformation mechanism and, as will be discussed, a source of additional dislocation slip directions. Although the twinning greatly affects the microstructure, dislocation slip may be considered the primary mode of deformation.

(d) Twin and dislocation interactions

Five Independent Slip Systems (ISS). Dislocation slip involving ⟨010⟩ dislocations will provide only three ISS, whereas five ISS are required for general plastic deformation of polycrystalline materials. As previously discussed, mechanical twinning on the various {114} planes alone could provide the B2 crystal structure with sufficient ISS. A single grain within a polycrystalline matrix must undergo an arbitrary shape change in order to deform homogeneously with the surrounding grains. Presuming that grain boundary sliding does not occur, different regions of that individual grain must undergo shearing on five different ISS in order to maintain grain boundary stability and prevent crack nucleation at triple points and unfavorable grain boundaries [34]. Some particular grains may be oriented such that slip in one slip system alone may account for most of the deformation within the greater part of those particular grains. For the severe deformation (40%) experienced by this material, five ISS must be activated in most grains. However, some of the ISS may only be activated locally near grain boundaries and may not be readily observed.

Since dislocation slip is two (2) ISS deficient, at least two mechanical twinning systems would be expected to be activated in a typical grain. Although some grains exhibit cross twinning, the typical grain in the 30 and 40% deformed samples exhibits only one set of parallel twin planes. Thus the twinning itself provides only one additional slip system, implying a total of only four (4) ISS are activated. Some deformation studies have suggested that four (4) ISS are sufficient in specific material systems [35, 36], but the large elongations obtained for $Ti_{50}Ni_{47}Fe_3$ indicates five (5) ISS should be necessary.

Three possible accommodations of this "missing" fifth ISS are suggested. TEM shows that some grains exhibit very fine twinning near a triple point, where the strain requirements are more stringent. Secondly, many grains exhibit parallel twins which curve as they approach a grain boundary. Mechanical twinning at different angles, due to crystallographic planes being "bent" by the presence of many dislocations, may provide the necessary strain to keep grain boundaries intact. These curved twins may also indicate that some grain rotation is occurring during swaging. Grain rotation is further substantiated by the observation of many grains with the $\{\bar{1}\bar{1}1\}$ matrix and {110} twin orientation parallel to the swaging direction, as was noted in the Characterization section and as will be discussed further in the next section. The observation of "curved twins" could also be an artifact of the severely bent nature of the metallic TEM foils.

The last and most likely explanation of the "missing" fifth ISS is that the mechanical twinning provides new dislocation slip directions. In the twinned region of material, three (3) new ⟨100⟩ directions exist. Thus three different ISS are present in the twin compared to those present in the matrix of the grain. Activating different slip systems in the neighboring twin and matrix may allow for general shape changes. A particular twin would not grow too large as a large single twinned region would itself then require five (5) ISS to deform. Although some initial deformation may occur via only dislocation slip, significant deformation requires dislocation slip and mechanical twinning to occur together.

Strain controlled twinning. The increase in both twin density and dislocation density with an increase in cold working (and flow stress) is substantiated by two observations. First, at least some twinning occurs after significant dislocation formation. In other words twin boundaries may pass through a tangled dislocation network as the twin is forming. Secondly, the dislocation density continues to significantly increase even after twinning has begun to occur. Both the dislocation density and the twin density continue to increase with subsequent deformation and work hardening.

Often mechanical twinning occurs after a particular stress level is attained, with continued twinning occurring without significant increase in stress [30, 37]. In the present material, however, twinning occurs during all stages of work hardening. Additionally, twinning occurs (with dislocation slip) at both room temperature and at 500°C (Fig. 10 and Ref. [13]). Mechanical twinning is required in conjunction with dislocation slip in this intermetallic, independent of the extent of work hardening and of the temperature of deformation. (It is noted that studies of other B2 structures deformed at high temperature have indicated the presence of additional slip systems [22, 38].) If there is a CRSS tor twinning, it apparently is similar to the CRSS for dislocation slip in TiNi, increases similarly with work hardening, and decreases similarly as the temperature increases.

In most materials where multiple modes of deformation are possible, the deformation mode requiring a lower stress at a particular strain rate and/or temperature will dominate. This is referred to as "stress-controlled" deformation and is likened to an isostress loading condition for a composite. In the case of TiNi, both twinning and dislocation slip occur together at various stress levels and temperatures. This synchronous occurrence of two deformation modes is likened to an isostrain loading condition in a composite. The "strain-controlled" twinning results as a direct consequence of the necessity of 5 ISS for plastic deformation.

The TEM observation of many grains in the 30 and 40% deformed material with $\{\bar{1}\bar{1}1\}$ matrix $\parallel$ $\{110\}$ twin orientations that are parallel to the swaging direction indicates that some grain rotation has occurred to preferentially orient the originally randomly oriented grains. TEM alone may not determine how the grain rotation is accounted for during deformation, but the following scenario is speculated. A randomly oriented grain may deform via dislocation slip. Passage of many dislocations makes the orientation of the grain rotate toward the swaging axis. After much deformation, the grain will have an orientation between the three $\langle 100 \rangle$ slip directions, i.e. a $\langle 111 \rangle$ orientation. When the grain is oriented with $\langle 111 \rangle$ parallel to the swaging direction, the $(\bar{1}\bar{1}4)$ plane will be close to 45° from the swaging direction, allowing a large resolved shear stress on the twinning plane. The twinned region will have the $\langle \bar{1}\bar{1}0 \rangle$ direction parallel to the swaging direction, as observed by electron diffraction. In this configuration, the twinned region will have two new $\langle 100 \rangle$ directions at $\sim 45°$ to the swaging direction, and dislocation slip within the twinned region will be optimized. Since the extent of grain rotation is a function of total strain, having grain rotation in conjunction with mechanical twinning implies the twinning to be "strain controlled".

Dislocations involved in shuffle of complex twinning. Goo's model [9] for (114) twinning accommodates the required shuffling by adding rows of vacancies on alternating (110) planes at each twin boundary. The shuffle, $\mathbf{s} = \mathbf{a}_0/2[00\bar{1}]$, occurs in the same direction as the Burgers vector of the slip dislocations. Since a high density of $\langle 100 \rangle$ type dislocations are present in the cold worked material (Fig. 3) prior to most twinning, these dislocations may help accommodate the twin formation and the associated shuffle, rather than being a hindrance. It has not yet been established whether the shuffling that is required for (114) twinning coincides with or occurs after the shearing part of the twinning process.

(e) Thermo-mechanical strengthening

The present intermetallic compound exhibits appreciable ductility, such that even after significant strain hardening some ductility is retained. However, heat treatments after cold working produce a structure with additional ductility as well as an increased strength over that of the annealed material. For example, 40% cold working results in a three-fold increase in strength as compared to that of the fully annealed material. As might be expected, this as-worked material has little remaining ductility. Yet, a 600°C anneal for 1 min increases the ductility to greater than 20% without sacrificing the majority of this increased strength. As will be discussed in this section, the superior mechanical properties of the cold worked and then heat treated alloy can be directly related to the substructure observed [example: Fig. 9(a)]. Interpreting the TEM micrographs determines the substructure, in turn, to be dependent on the extent of mechanical twinning.

The case of the 10% cold worked material, which exhibited little mechanical twinning, is considered first. Annealing this cold worked structure basically reduces the dislocation density, comparing Figs 3 and 8. Some recovery occurs by the lining up of dislocations, suggestive of subgrain boundaries. However, further annealing [comparing Figs 8(a) and (b)] results in a further reduction of the dislocation density. In addition, the spacing between dislocation rows increases with annealing time. This implies that if subgrain boundaries are present, they are not stable, with the subgrain size increasing with annealing time. The tensile tests performed on these annealed (after 10% cold work) samples also show that greater annealing time just results in a lower yield strength. No fine substructure is observed in any sample annealed after 10% cold swaging.

Whereas the dislocated structure was not a hindrance to the formation of mechanical twins in the 30 and 40% deformed samples, short anneals of the cold-worked structure of dislocations and twins, results in recovery of the dislocations but not of the twin boundaries. Comparing the as-worked microstructure in Fig. 5(a) to the annealed microstructure of Fig. 9(a) indicates that the twin boundaries are stable, whilst the dislocation density has decreased. In some regions the dislocations appear to have lined up but always within the confines of the twin boundaries which therefore provide a hindrance to dislocation recovery. Long annealing of the 30% cold worked material eventually results in a loss of twin boundary integrity across the whole grain [Fig. 9(b)]. The resulting substructure is quite stable, with the previous twin boundaries acting as part of the subgrain boundaries. The mechanical testing results plotted in Fig. 12(a) determine that further annealing results in no substantial loss of strength and indicate the structural stability of these fine subgrains. The greater twinning density in the 40% (as compared to the 30%) cold worked material provided the former with a higher yield strength after annealing. The finer is the spacing between twins, the finer is the substructure after annealing and the higher is the resulting yield strength as a result of subgrain-size strengthening [Fig. 12(b) and Table 1]. Again, this substructure is stable with longer anneals, with the subgrain size comparable to the twin spacing in the as-worked material.

Greater cold working results in a finer twin density, which, when annealed, results in a fine subgrain structure with a correspondingly increased mechanical strength. The interaction of two deformation modes to provide a means of thermo-mechanically strengthening an alloy is an important metallurgical consideration. Just as a composite may be tailored for desired properties, the TiNi intermetallic may be tailored for desired strength/ductility. A higher strength B2 structure provides a greater strength differential between the austenite and martensite structures, which, in turn, enhances the Shape Memory Effect in TiNi alloys.

Although the B2 structure exhibits only 3 independent slip systems, the ability to mechanically twin provides this intermetallic with significant room temperature ductility. Why this particular B2 material mechanically twins, providing ductility and the ability to be thermo-mechanically strengthened, is not well understood. The effects of stacking fault energy, number of free electrons in the structure, third element additions, etc. on mechanical twinning may be studied. Future attempts to enhance mechanical twinning in other intermetallic compounds may be considered.

CONCLUSIONS

1. Mechanical deformation in TiNi is observed by TEM to occur by a combination of dislocation slip and mechanical twinning.

2. The Burgers vector of the dislocations are shown to be $\langle 100 \rangle$, which provides only three independent slip systems.

3. The complex twinning mode is the $\{114\}\langle 22\bar{1} \rangle$ type, as found previously by Goo *et al.* [9].

4. Twinning within a particular grain occurs on only one set of parallel planes, thus providing a fourth ISS. However, the newly oriented twins can in turn undergo dislocation slip on additional slip systems. Thus polycrystalline TiNi can undergo compatible plastic deformation with significant room temperature ductility.

5. Post-work annealing causes dislocation recovery within the confines of the width of the twins, resulting in fine stable subgrains and an improved combination of yield strength and ductility in this intermetallic.

6. The concurrence of mechanical twinning with dislocation slip in other superlattice structures may provide a means of thermo-mechanically processing other intermetallic alloys.

Acknowledgements—This research was conducted as part of the Ph.D. thesis of the first author at Stanford University. Support for this research by Raychem Corporation is gratefully acknowledged. Also helpful discussions with Alain Schwartzman, Bill Nix, Vikram Jayaram, and Dave Barnett are most appreciated.

REFERENCES

1. S. P. Gupta and A. A. Johnson, *Trans. Japan Inst. Metals* **14**, 292 (1973).
2. G. M. Michal and R. Sinclair, *Acta crystallallogr. B* **37**, 1803 (1981).
3. K. M. Knowles and D. A. Smith, *Acta metall.* **29**, 101 (1981).
4. K. Otsuka, T. Sawamura and K. Shimizu, *Physica status solidi* (a) **5**, 457 (1971).
5. C. M. Wayman, *Shape Mem. Eff. Conf. Proc.*, China, p. 59 (1986).
6. C. T. Liu and J. O. Stiegler, *Science, N.Y.* **226**, 636 (1984).
7. T. Kawabata, M. Tadano and O. Izumi, *Scripta metall.* **22**, 1725 (1988).
8. K. H. Hahn and K. Vedula, *Scripta metall.* **23**, 7 (1989).
9. E. Goo, T. Duerig, K. Melton and R. Sinclair, *Acta metall.* **33**, 1725 (1985).
10. J. L. Proft, W. J. Moberly, T. Duerig and R. Sinclair, *TMS-AIME Annual Meeting*, Pheonix (1988).
11. G. M. Michal, Ph.D. thesis, Stanford Univ. (1979).
12. A. R. Pelton, E. H. Huang, P. Moine, R. Sinclair and M. A. Noack. To be submitted.
13. W. J. Moberly, *Ultramicroscopy* **30**, 395 (1989).
14. W. J. Moberly, J. L. Proft, T. Duerig and R. Sinclair. In preparation.
15. M. H. Yoo, J. A. Horton and C. T. Liu, *Acta metall.* **36**, 2935 (1988).
16. M. J. Mills, N. Balluc and H. P. Karnthaler, *Mater. Res. Soc. Proc.* (edited by C. T. Liu, A. I. Taub, N. S. Stoloff and C. C. Koch), Vol. 133, p. 203 (1989).
17. G. W. Groves and A. Kelly, *Phil. Mag.* **8**, 877 (1963).
18. R. Von Mises, *Z. Ang. Math. Mech.* **8**, 161 (1928).
19. G. I. Taylor, *J. Inst. Metals.* **62**, 307 (1938).
20. M. H. Loretto and R. J. Wasilewski, *Phil. Mag.* **23**, 1311 (1971).
21. J. Bevk, R. A. Dodd and P. R. Strutt, *Metall. Trans.* **4**, 159 (1973).
22. C. H. Lloyd and M. H. Loretto, *Physica status solidi* **39**, 163 (1970).
23. D. L. Yaney, A. R. Pelton and W. D. Nix, *J. Mater. Sci.* **21**, 2083 (1986).
24. F. Laves, *Naturwissenschaften* **39**, 546 (1952).
25. M. L. Green and M. Cohen, *Acta metall.* **27**, 1523 (1979).
26. E. Goo, *Scripta metall.* **22**, 1079 (1988).
27. V. Jayaram, *Scripta metall.* **22**, 741 (1988).
28. E. Goo and K. T. Park, *Scripta metall.* To be published.
29. U. F. Kocks and D. G. Westlake, *Trans. Am. Inst. Min. Engrs* **239**, 1107 (1967).
30. H. Suzuki and C. S. Barrett, *Acta metall.* **6**, 156 (1958).
31. R. W. Cahn, in *Deformation Twinning* (edited by R. E. Reed-Hill), Gordon & Breach, New York (1964).
32. J. P. Hirth and J. Lothe, *Theory of Dislocations*, 2nd edn. Wiley, New York (1982).
33. W. J. Moberly, A. R. Pelton, T. Duerig and R. Sinclair, in preparation.
34. V. Jayaram, *Acta metall.* **35**, 1307 (1987).
35. R. L. Fleischer, *Acta metall.* **35**, 2129 (1987).
36. J. D. Livingston and B. Chalmers, *Acta metall.* **5**, 322 (1957).
37. T. H. Blewitt, R. R. Coltman and J. K. Redman, *J. appl. Phys.* **28**, 651 (1957).
38. D. L. Yaney, Ph.D. thesis, Stanford Univ. (1986).